Laser and Particle Beams (2003), *21*, 411–418. Printed in the USA.

DOI: 10.1017/S0263034603213197

Shock-tube experiments on Richtmyer–Meshkov instability growth using an enlarged double-bump perturbation

D.A. HOLDER, A.V. SMITH, C. J. BARTON, AND D.L. YOUNGS
Atomic Weapons Establishment, Reading, Berkshire, United Kingdom
(RECEIVED 12 April 2002; ACCEPTED 4 April 2003)

Abstract

This article reports on the latest experiments in the series of Richtmyer–Meshkov instability (RMI) shock-tube experiments. Previous work described a double-bump experiment that evidenced some degree of unrepeatability. The present work features an enlarged perturbation introduced to improve repeatability. In common with the previous work, the experiments were conducted at shock Mach number 1.26 (70 kPa overpressure), using the Atomic Weapons Establishment 200 × 100 mm shock tube with a three-zone test cell arrangement of air/sulphur hexafluoride/air. The sulphur hexafluoride gas (SF_6) was chosen for its high density (5.1 relative to air) providing an Atwood number of 0.67. Gas separation was by means of microfilm membranes, supported by fine wire meshes. A double-bump perturbation of two-dimensional geometry was superimposed on the downstream membrane representing a 0.6% addition to the dense gas volume. Visualization of the turbulent gas mixing was by laser sheet illumination of the seeded SF_6 gas using a copper vapor laser pulsing at 12.5 kHz. Mie scattered light was recorded using a 35-mm rotating drum camera to capture a sequence of 50 images per experiment. Sample experimental results shown alongside corresponding three-dimensional hydrocode calculations highlight the problems in both analysis and comparison caused by multiple scattering arising from the necessary use of a high seeding concentration. Included is a demonstration of the effectiveness of introducing into the hydrocode a Monte Carlo-based simulation of the multiple scattering process. The results so derived yield greatly improved qualitative agreement with the experimental images. Quantitative analysis took the form of deriving relative intensity data from line-outs through experimental images and their code equivalents. A comparison revealed substantial agreement on major features.

Keywords: Compressible turbulent mixing; Laser sheet technique; Mie scattering; Multiple scattering; Richtmyer–Meshkov instability

1. INTRODUCTION

This article describes recent experiments in the series of Richtmyer–Meshkov instability studies conducted on the Atomic Weapons Establishment (AWE) 200 × 100 mm shock tube. The laser sheet technique was used to image the mixing process across the two interfaces of a dense gas region bounded by air on either side. The experiments featured a shock Mach number of 1.26 and an Atwood number of 0.67. Such experiments are conducted to provide experimental data that, in conjunction with three-dimensional (3D) numerical simulation, serve to validate two-dimensional (2D) turbulent mix models being developed at AWE. These models are used in hydrocodes for modeling the physics of implosion phenomena.

The experiments described here investigated the influence on the Richtmyer–Meshkov instability mixing across both gas interfaces caused by the superimposition of a double-bump perturbation on the downstream interface. They therefore involve the mutual interaction between two 2D perturbations, the results of which can be considered to be 2D on average. The amplitude of the bumps was chosen so as to improve upon the quality and repeatability of the results from earlier experiments using a smaller amplitude (Smith *et al.*, 1997, 1999).

Qualitative comparisons between experimental images and those obtained from the AWE TURMOIL 3D computational code calculations are presented, showing good agreement, apart from a distinct loss of clarity of mix features in

Address correspondence and reprint requests to: D.A. Holder, Bldg. H27, AWE, Aldermaston, Reading, Berkshire, RG7 4PR, Great Britain. E-mail: david.holder@awe.co.uk

the laser sheet images. The cause of the diffuse appearance of the images is known to be due to multiple scattering that stems from the use of a high seeding concentration. To investigate the problem, a Monte Carlo simulation of the scattering process was devised. This was applied as a post-processing technique to the code calculations so that both the gas mixing and the light scattering processes underlying the formation of an experimental image were represented. It resulted in significantly improved visual comparison of images from code and experiment. It also enabled quantitative analysis to be performed, in the form of relative intensity line-out data.

Reference is made in Section 7 to the proposed use of intensified CCD (ICCD) cameras to allow the use of significantly lower seeding levels and anticipated obviation of the multiple scattering problem.

A complete 50-image video sequence comparing images from the experiment with those from the code (without Monte Carlo postprocessing) provides improved visualization of the mixing process. This is available in the shock tube pages on the AWE website: www.awe.co.uk/main_site/scientific_and_technical/featured_areas/hydrodynamics/.

2. DESCRIPTION OF THE EXPERIMENT

A general form of the experiment has already been reported by Smith *et al.* (1997, 1999). A brief explanation follows.

A conventional shock tube is used to generate a plane air shock (Mach No. 1.26) of 70 kPa constant overpressure and 7 ms duration. This passes into a transparent test cell comprising three gas zones (Fig. 1), 1 and 3 containing air, and 2 containing a dense gas (sulphur hexafluoride, SF_6; relative density 5.1) seeded with an olive oil aerosol. The gases are separated by microfilm membranes supported by fine wire meshes. The double-bump perturbation (two-dimensional) on the downstream membrane is achieved by the combined use of profiled test cell components and additional transverse (control) wires. The gases are initially at atmospheric pressure.

Figure 1 illustrates the basic experimental arrangement. Interrogation of the turbulent mixing was by means of the pulsed laser sheet technique, recording the Mie scattered laser light from seeding particles in the SF_6 gas. The output beam from a pulsed copper vapor laser is formed into a sheet of 1 to 2 mm thickness that enters the test cell via a central vertical slit in the end plate. The SF_6 was seeded using an atomiser containing olive oil. The resultant aerosol scatters light from the laser sheet to a 35-mm rotating drum camera (rotating at 250 ms^{-1}), viewing from 90° and focused on the sheet. This records fifty sequential images of the mixing process as interrogated by the laser sheet. These spanned the range of interest from shock arrival at the first interface (0 ms) through to late stage mixing (4 ms). Black and white 400 ASA film was used and processed to 6400 ASA equivalent.

The test cell is of demountable construction to facilitate installation of different profiled sections. The roof and floor of the dense gas zone feature large diameter poppet valves to facilitate complete filling with dense gas while avoiding membrane failure caused by excessive internal pressure. The valves are closed by solenoids during the firing sequence.

Pressure transducers record the shock passage along the shock tube, one of which provides a signal for synchronizing the laser and camera operation with shock propagation.

A pulsed copper vapor laser (approximately 5 mJ energy per pulse) provided dichroic laser light illumination, wavelengths 511 and 578 nm in an approximate energy ratio 2:1. Operation in unstable cavity mode, essential for sheet-

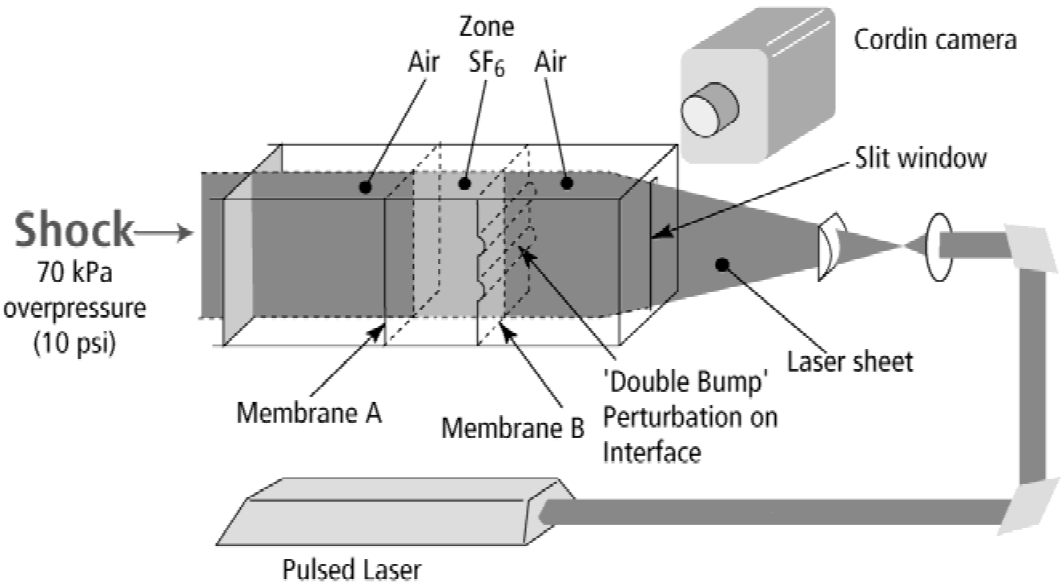

Fig. 1. Schematic of the experimental configuration.

https://doi.org/10.1017/S0263034603213197 Published online by Cambridge University Press

forming applications, slightly reduces the available pulse energy. The laser is operated at a pulse repetition rate of 12.5 kHz with a pulse duration of approximately 30 ns.

3. PERTURBATION PROFILE

This is one of a series of perturbation profiles modeling the mixing of gases in a three-zone experimental environment. An enlarged double bump was chosen to circumvent problems with reproducibility in a previous double-bump experiment (Smith *et al.*, 1999). These problems arose through inadequate control over membrane shrinkage during the process of drying and consequent unavoidable deformations along the tensioning (control) wires spanning the 100-mm width of the test cell. With the earlier bump amplitude of only 3 mm (i.e., protrusion from the plane interface), the observed midway deflection (sag) of typically 1 mm proved unacceptable. Doubling the perturbation amplitude to 6 mm (Fig. 2) and exercising tighter control over wire tensioning and membrane drying reduced such deficiencies to an acceptable level. It is noted that the additional volume of dense gas due to the double-bump perturbation is 0.6% of the total.

4. EXPERIMENTAL AND CODE RESULTS

In Figure 3, columns 1 and 2, show eight sample original photographic images from one experiment, paired with their corresponding computational results. The latter represent central vertical plane "slices" through a TURMOIL 3D turbulent mix code calculation with intensity proportional to partial SF_6 gas density; shocks are clearly revealed.

The specific times selected, from the 50 recorded experimentally, are as follows: 0 ms, showing the initial position of the dense gas, awaiting shock arrival at the left-hand boundary; 0.5 ms, showing the passage of the incident shock; 1.3 ms, showing the phase inversion of the bump perturbations and presence of a rarefaction wave travelling upstream (code only); 1.9 ms, showing the passage of the reflected shock from the end plate; 2.2 ms, showing the passage of second reflected shock from the end plate (code only); 2.7 ms, showing axial compression of bubble cavities and spike growth; 3.3 ms and 4.0 ms, showing the late time growth of the mix region.

The TURMOIL 3D code used to model the experiments is a semi-Lagrangian calculation. The *x*-direction (along the shock tube) mesh moves with the mean fluid velocity; the y- and z-meshes are fixed. The 3D zoning used is $400 \times 320 \times 160$. The numerical technique is a simple finite volume method in which, for each time step, there is a Lagrangian phase followed by a rezone phase that uses the monotonic advection method of van Leer. It is an example of the MILES technique, and the suitability of this approach for Rayleigh–Taylor mixing was discussed by Linden *et al.* (1994).

Perfect gas equations of state are used ($\gamma = 1.076$ for SF_6, $\gamma = 1.401$ for air). Initial perturbations were applied to both inner and outer air/SF_6 interfaces to represent the effect of membrane rupture. The random amplitude (ζ) perturbations were of the form

$$\zeta(y,z) = S \sum_{m,n\geq 0} \cos\frac{m\pi y}{H}\left(a_{mn}\cos\frac{2n\pi z}{L} + b_{mn}\sin\frac{2n\pi z}{L}\right).$$

The wavelength, λ, for mode (m,n) is given by

$$\frac{1}{\lambda^2} = \frac{1}{\lambda_y^2} + \frac{1}{\lambda_z^2}$$

where

$$\lambda = \frac{2H}{m}, \qquad \lambda_z = \frac{L}{n}.$$

H is the height and L is the width of the shock tube. Modes are included for which $0.5\text{ cm} < \lambda < 5\text{ cm}$ and in that case, the coefficients are chosen from a Gaussian distribution with unit *SD*. Finally the scaling factor S is chosen to give $\sqrt{\langle\zeta^2\rangle} = 0.01$ cm.

The small-scale debris visible in the experimental images provides evidence of the effectiveness of the wire meshes in fragmenting the membranes. The code results in column 2 are shown without modification for multiple scattering. Visual comparison with experiment shows general agreement in respect to size and position of the large-scale features. The diffuse appearance of the experimental images is readily apparent, to the extent that while incident shocks are visible, rarefaction waves (e.g., 1.3 ms) are not.

Following reporting of the earlier series of experiments (Holder, 1998), it was realized that the phenomenon of multiple scattered light recorded in the images rendered extraction of quantitative mix data (i.e., gas composition and

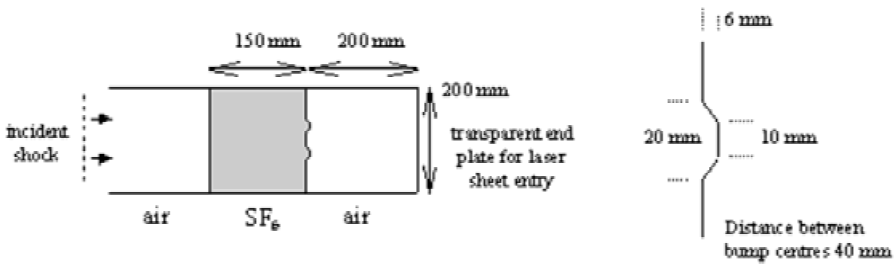

Fig. 2. Double-bump perturbation on the downstream boundary.

https://doi.org/10.1017/S0263034603213197 Published online by Cambridge University Press

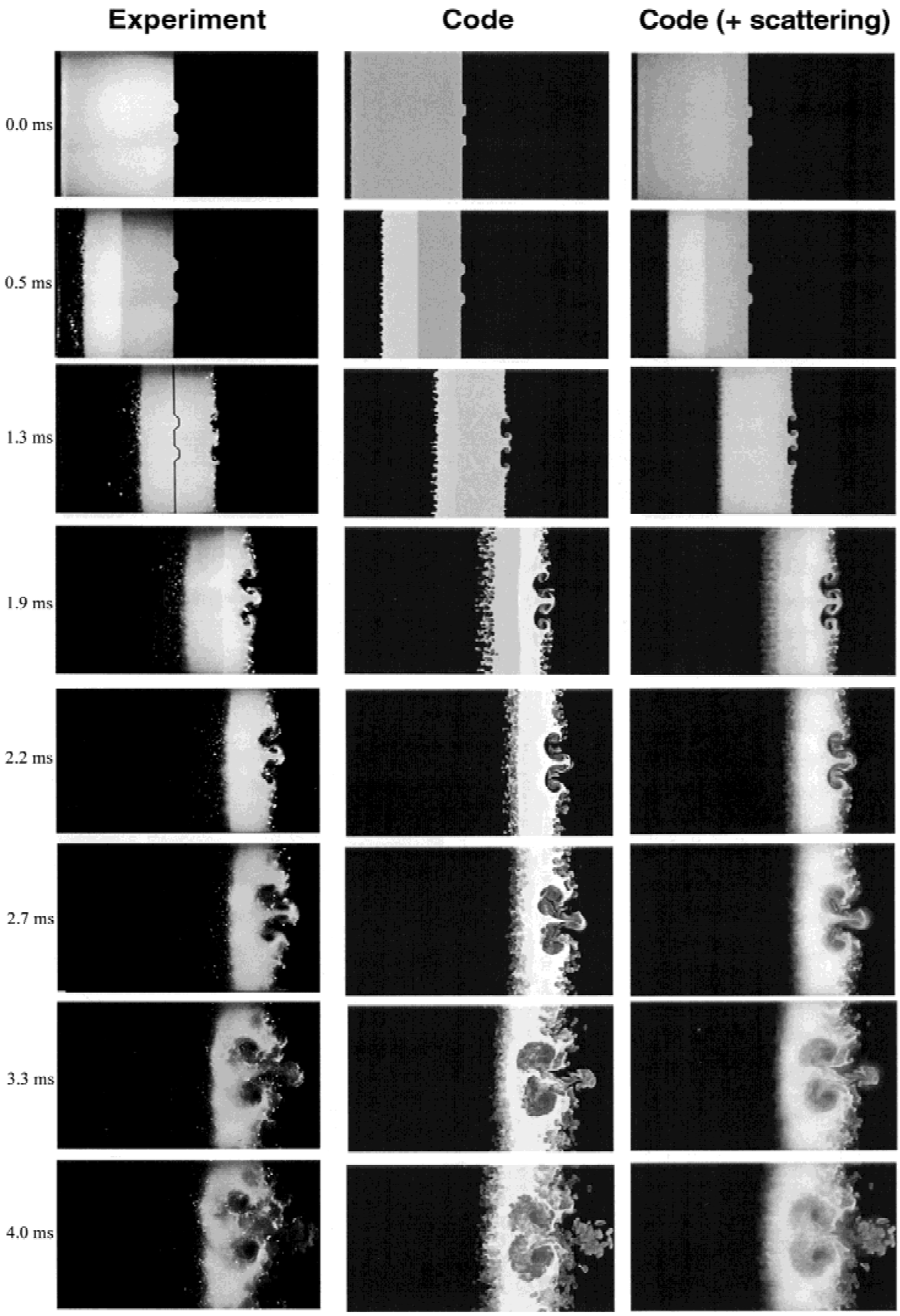

Fig. 3. Sample photographic images and corresponding computational code results (0–4.0 ms).

https://doi.org/10.1017/S0263034603213197 Published online by Cambridge University Press

densities) an impossible task. Therefore, while pursuing alternative or modified imaging techniques, it was decided as an interim measure to adapt the *code* results to include representation of the multiple scattering process. The results in column 3 are obtained by applying a multiple scattering postprocessing technique to the results of column 2: this is a Monte Carlo routine as presented at the last International Workshop on the Physics of Compressible Turbulent Mixing (Giddings *et al.*, 1999). Essential input data for its development was derived from analysis of supporting laser sheet experiments and analysis.

In column 3, the results are visibly more comparable with experiment, though with the loss of structure detail formerly present.

5. MULTIPLE SCATTERING: RECOGNITION AND SIGNIFICANCE

Laboratory investigations in the form of ad hoc laser sheet experiments were performed to provide empirical support for development of the Monte Carlo simulation. A specific requirement was to establish a value for the mean free path for photon scattering within the seeded SF_6 gas, undiluted by air. Gas penetration distances of up to 400 mm were investigated. The findings revealed a mean free path length of around 50 mm, dependent on the initial seeding concentration: This decreases under shock compression but increases as mixing with air develops. In the double-bump experiment, photons from the laser sheet enter centrally and penetrate up to a maximum of 150 mm into the seeded gas (i.e., the distance between the membranes) followed by a further mean distance of 50 mm in order to reach the test cell windows. Mean photon travel within the seeded gas is therefore typically several times the mean free path. This observation clearly undermined the original assumption that the Mie scattering process was adequately described by primary (first order) scattering alone.

An immediate consequence is that multiple scattering gives rise to an attenuation curve featuring a distinct shift in the position of maximum intensity away from the entry plane. This is due to enhancement of the light intensity in the forward direction initially overriding the normal decay process. The complexity of the scattering process underlying such modification, particularly in a varying (spatial, temporal and pressure) two-component gas field (one gas seeded), defied attempts to derive analytical equations required to extract the required gas data. [It is noted that an analytical treatment (Giddings, 1999) of multiple scattering superseded the concept of the Monte Carlo approach but became overly complex at the stage of second order scattering.]

The Monte Carlo technique involved has been previously reported (Holder *et al.*, 2001); however, a brief summary is given. It uses Mie theory for the mean scattering cross section and assumes a known droplet size distribution and concentration. An input of 800,000 particles represents a laser sheet pulse and the model calculates up to 10th order scattering with only the first scatter necessarily within the plane of the laser sheet. The Monte Carlo code is applied to the air/SF_6 gas mix distribution, as determined by the TURMOIL 3D code, producing an image that incorporates multiple scattering. Figure 4 illustrates this.

A computational particle represents a packet of photons of energy W. Each particle is forced to have n (~ 10) collisions and the scattered light intensity contribution to the image for each order of collision is calculated, where:

where

W_n = Particle energy after collision n at point P_n,

τ_n = Number of mean free paths along exit path $P_n E_n$,

$W_n e^{-\tau_n}$ = energy lost from the system, and

$W_{n+1} = W_n(1 - e^{-\tau_n})$, energy after $n+1$ collisions at a randomly chosen point P_{n+1}.

Figure 5 provides results from the Monte Carlo simulation. It illustrates the contribution to the overall scattered light intensity of each successive scattering order, with evidence that orders approaching 10 contribute only minimally (only 8 orders are shown for clarity). Higher orders were accordingly ignored in formulating the Monte Carlo simulation subsequently used to generate the modified code images. The second figure demonstrates the success of the Monte Carlo simulation in modeling the data from an ad hoc experiment featuring a 40-cm-long seeded SF_6 gas zone.

The significance of multiple scattering in the double-bump series of experiments manifests itself as two problems. First, it causes "fogging" of the laser sheet images (as evident in Figure 3); resolution is thereby lost, so impairing the ability to qualitatively compare with code results. The second more restricting implication is that it effectively defies quantitative analysis and hence extraction of the gas mixture data required for code validation.

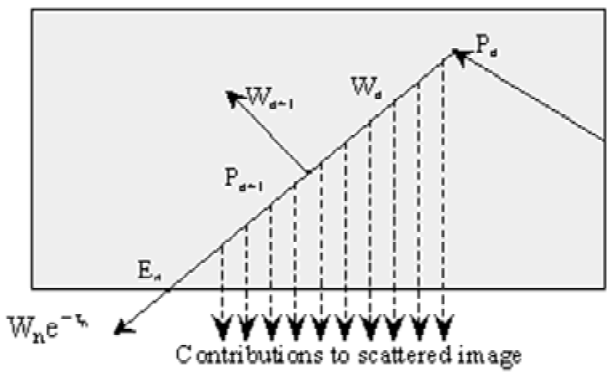

Fig. 4. Plan view illustration of how the Monte Carlo code calculates a scattered image.

https://doi.org/10.1017/S0263034603213197 Published online by Cambridge University Press

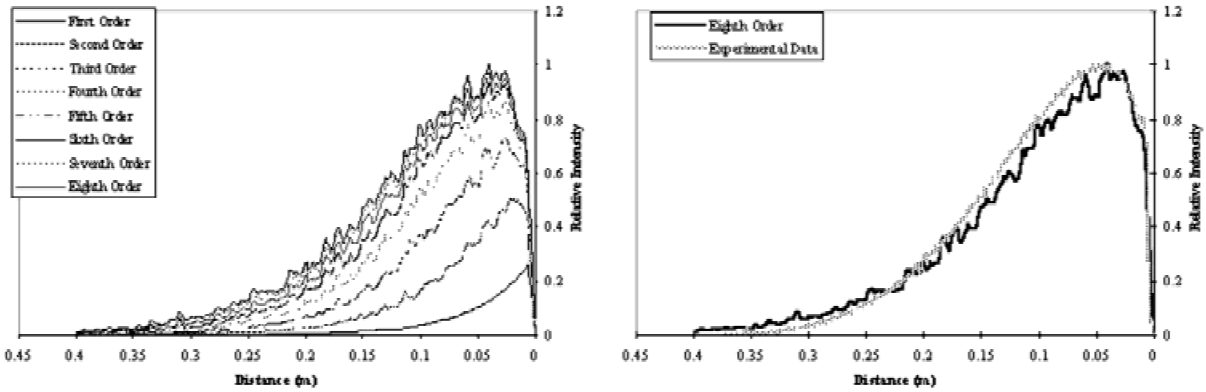

Fig. 5. Contribution of multiple orders of scattering and the comparison between experimental and Monte Carlo code data.

6. ANALYSIS

As explained in Section 4, the code results (Fig. 3, column 3) have been modified with the Monte Carlo postprocessor partly to facilitate qualitative comparison with experiment but also to enable a measure of quantitative analysis to be undertaken. The modification, essentially a "smearing" process, however, loses the singular relationship between image intensity and local SF_6 gas concentration. The analysis therefore became limited to a pseudo-validation of the modified code by experiment, involving comparison of intensity line-outs through images, though without the capability of direct linkage to gas properties.

Several images were selected for analysis: detailed results from one will suffice to demonstrate the comparison between experimental and modified code line-out data. Figure 6 shows the results for the time 2.7 ms. The zero (0 cm) position represents the location of the upstream boundary of the dense gas region, and the end termination of the test cell is at 350 mm. The line-out positions were chosen to produce horizontal line-outs through the center of the perturbations and along the test cell axis. These line-outs show close agreement between code and experiment when the Monte Carlo routine is applied to the hydrocode results.

7. DISCUSSION

This work has been shown to support mix model code development by providing experimental images that qualitatively validate the mixing process.

It is anticipated that the problems of multiple scattering can be overcome by reducing the SF_6 seeding concentration by between 1 to 2 orders of magnitude, such that primary scattering dominates the process. This will, however, correspondingly reduce the light intensity levels such that unless the laser power is boosted by a corresponding factor, or alternatively the viewing area is reduced, then photographic film will no longer provide a suitable recording medium. Accordingly, an intensified CCD camera has been procured, which has been demonstrated as satisfying sensitivity and gating requirements. This single camera, yet to be fully evaluated, is expected to allow the acquisition of one preshock and one postshock image with a minimal multiple scattering component. It is anticipated that subsequent quantitative analysis should pose no inherent difficulties and will significantly benefit from elimination of the need for digitization and correction for film characteristics.

Of increased concern with reduced seeding concentration is possible image interference due to the presence of fragmented membrane particles. The present seeding material is olive oil dispersed as droplets, with a mean in the range 0.3 to 0.8 μm diameter resulting in Mie scattering. Imaging of the mix region records not only the laser light scattered from the seeding particles, but additionally any reflections from the membrane fragments. The contribution from the latter in the images presented in this report is insignificant. However, with the proposed reduction in seeding concentrations, the relatively higher level of reflected light from the fragments may obscure areas of the mixing region. It is therefore proposed that the seeding particles be replaced by fluorescent particles that absorb the incident laser radiation and reemit at a different wavelength. The use of a selective notch filter on the camera lens would allow transmission of light at the fluorescent wavelength while blocking the incident and reflected laser light. By so excluding unwanted light (i.e., from multiple scattering and reflection from the membrane fragments), improvements should be expected in both image quality and ease of quantitative data extraction.

In the absence of multiple scattering, quantitative comparison between experimental images and simulations will be achieved. Without multiple scattering, the light intensity recorded by the camera will be directly proportional to the seeding agent concentration and hence the dense gas concentration. Therefore the intensity images will, after calibration, be compared directly with the concentration information from the simulations. A map of differences could then be

https://doi.org/10.1017/S0263034603213197 Published online by Cambridge University Press

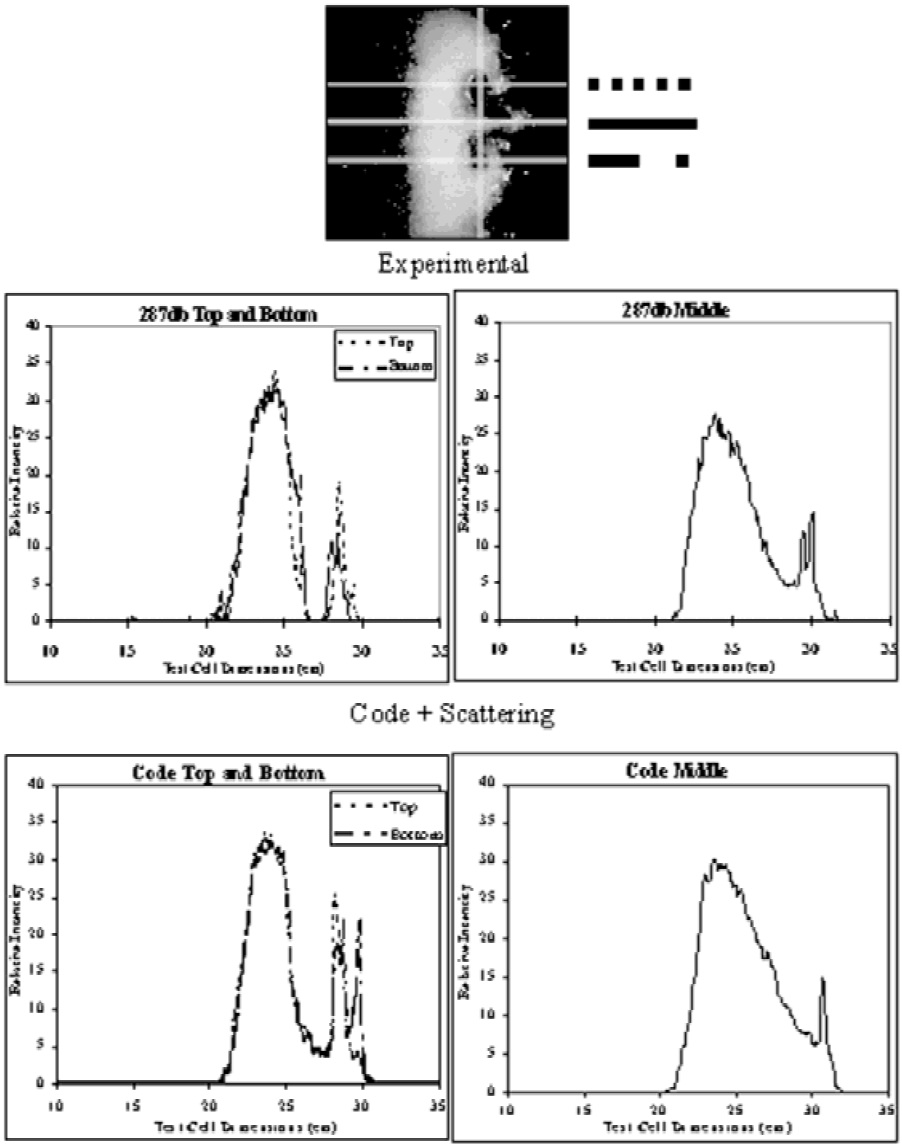

Fig. 6. Comparison of experimental and code line-outs for 2.7 ms.

produced and those differences quantified. A figure of merit for the whole images region or separate regions of interest could then be established as a measure of agreement between the experiments and simulations.

8. CONCLUSIONS

This article reports the second series of double-bump perturbation mix experiments. Improved success in quality and repeatability over the previous series has been demonstrated. This has resulted primarily from the enlargement of the perturbation. It is noted that the additional dense gas contained by the two bump perturbations is still small at only 0.6% of the total dense gas volume.

Since the first series, the existence and significance of the multiple scattering problem has been extensively investigated. A simulation of the process using a Monte Carlo routine has been developed, supported by ad hoc experiments, and then applied, as a postprocessor, to the results from the 3D numerical code simulation. It has resulted in close agreement with the experimentally observed development and distribution of large-scale features of the turbulent mix region. It has also provided indication of a high level of agreement in the limited quantitative analysis performed.

It must be noted that, due to multiple scattering, true validation of the experimental results has not been achieved. Nevertheless, close agreement has been observed between the modified code, incorporating multiple scattering, and experiment. It suggests that, accepting that the code calculations are derived from a two-stage process consisting of applying a multiple scattering (Monte Carlo) routine to a

https://doi.org/10.1017/S0263034603213197 Published online by Cambridge University Press

hydrocode calculation, the latter is appropriately modeling the experiment.

However, the two-stage process must be considered a less than ideal interim measure. The proposed solution involves a significant lowering of the seeding concentration, necessitating the use of ICCD camera systems to function at the low light levels expected. A single camera, providing one mix image per experiment, has accordingly been purchased and is currently undergoing evaluation. It is also proposed to replace the seeding particles with fluorescent particles and filter out the laser wavelength. This will then lead to a quantitative comparison between experiments and simulations.

REFERENCES

GIDDINGS, R., HOLDER, D.A., PHILPOTT, M.K. & YOUNGS, D.L. (1999). An investigation of the problem of multiple scattering from seeding particles in laser sheet turbulent mix visualization studies. *Proc. 7th Int. Workshop on the Physics of Compressible Turbulent Mixing*, pp. 22–27. (Meshkov, E., Yanilkin, Yu. & Zhmailo, V., Eds.). Sarov, Russia: RFNC-VNIIEF.

HOLDER, D.A. (1998). Explanation of the observed anomaly in the analysis of the photographic images from the shock tube experiments. Report No. AWE/HDFM/B/9812/910. Reading, Berkshire, UK: Atomic Weapons Establishment.

HOLDER, D.A., PHILPOTT, M.K. & YOUNGS, D.L. (2001). An investigation of the problem on multiple scattering from seeding particles in laser sheet studies of shock induced gas mixing. *Proc. 23rd Int. Symposium on Shock Waves*, pp. 1133–1139. (Lu, F.K., Ed.). Arlington, Texas: The University of Texas at Arlington.

LINDEN, P.F., REDONDO, J.M. & YOUNGS, D.L. (1994). Molecular mixing in Rayleigh–Taylor instability. *J. Fluid Mech.* **265**, 97–124.

SMITH, A.V., PHILPOTT, M.K., MILLAR, D.B., HOLDER, D.A., COWPERTHWAITHE, N.W. & YOUNGS, D.L. (1997). Shock tube investigations of the Richtmyer–Meshkov instability due to a single discrete perturbation on a plane gas discontinuity. *Proc. of the 6th Int. Workshop on the Physics of Compressible Turbulent Mixing*, pp. 480–485. Marseille, France: Imprimerie Caractère.

SMITH, A.V., HOLDER, D.A., PHILPOTT, M.K. & MILLAR, D.B. (1999). Notch and double bump experiments using the 200 × 100 mm linear shock tube. *Proc. 7th Int. Workshop on the Physics of Compressible Turbulent Mixing*, pp. 124–130. (Meshkov, E., Yanilkin, Yu. & Zhmailo, V., Eds.). Sarov, Russia: RFNC-VNIIEF.

https://doi.org/10.1017/S0263034603213197 Published online by Cambridge University Press